Enhanced Charge Storage of Ultrathin Polythiophene Films within Porous Nanostructures

Siamak Nejati, Thomas E. Minford, Yuriy Y. Smolin, and Kenneth K. S. Lau*

Department of Chemical and Biological Engineering, Drexel University, 3141 Chestnut Street, Philadelphia, Pennsylvania 19104, United States

ABSTRACT In a single step polymerization and coating, oxidative chemical vapor deposition (oCVD) has been used to synthesize unsubstituted polythiophene. Coatings have been conformally coated within porous nanostructures of anodized aluminum oxide, titanium dioxide, and activated carbon. Significant enhancement in charge capacity has been found with ultrathin polythiophene coatings that preserve the surface area and pore space of the nanostructures. Pseudocapacitors consisting of ultrathin polythiophene coated within activated carbon yielded increases of 50 and 250% in specific and volumetric capacitance compared with bare activated carbon. Devices were stable up to the 5000 cycles tested with only a 10% decrease in capacitance.

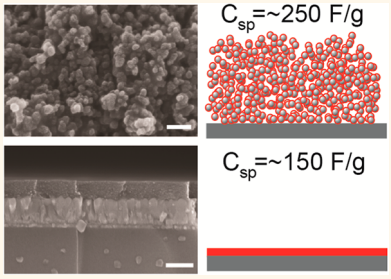

KEYWORDS: polythiophene · activated carbon · oxidative chemical vapor deposition (oCVD) · nanostructured electrode · pseudocapacitor

Conducting polymers as active materials for supercapacitors have gained significant attention and the efforts in using them in such devices have shown great promise.[1−3] These polymers have the ability to be p- and n-doped, and they have been shown to have high specific capacity, energy density and exceptional stability.[1] Using less costly and more readily available polymeric materials when compared to oxide-based materials like hydrous ruthenium oxide make them an excellent choice in enhancing charge capacity through Faradaic redox reactions that provide increased capacitance (pseudocapacitance).[4] Importantly, Simon and Gogotsi have proposed that the integration of ultrathin pseudocapacitive materials within porous carbon nanostructures could result in significant improvement in energy density and power density that can deliver both battery-like (high capacity) and capacitor-like (high rate) behavior in a single electrode.[5] For example, an ultrathin coating of manganese oxide within a carbon nanofoam and a layer-by-layer assembly of carbon nanotubes yielded significant increases in energy density compared with just the bulk oxide (~50 *vs* 100 F/g).[6,7] With conducting polymers, although they have suitable electrochemical charge storage capacity and reversibility, using liquid-based approaches to fabricate conducting polymer pseudocapacitors poses new challenges in materials integration, particularly with ultrathin coatings within high surface area capacitor electrodes, which consequently hinder device performance. The challenges are associated with a lack of intrinsic solubility of many conducting polymers in common solvents, and the presence of liquid surface tension that interferes with substrate wettability and conformal coating when working with polymer solutions. Most of the reports to date are limited to making planar electrodes or bulk composites, and in a few cases where the porous substrate was conductive enough, electrochemical synthesis was used for *in situ* polymerization.[1,2,8−11] Interestingly, when the polymer was made in the form of nanostructures or grown over carbon nanotubes, graphene oxide and within oxide nanostructures significant improvements in energy density compared to the bulk polymer have been reported.[8,10,12−15] Some of the reported capacitance values are far above the theoretical limit (350 F/g calculated assuming one charge for every three polymer repeat units based on the current understanding of the redox capacity of conducting polymers).[16] This discrepancy might be a result of the greater experimental

* Address correspondence to klau@drexel.edu.

Received for review May 8, 2013 and accepted May 19, 2014.

Published online May 19, 2014
10.1021/nn500007c

uncertainty introduced when a small mass of sample is used in the electrochemical measurements.[6,17]

There is great promise for achieving enhanced charge storage with building a pseudocapacitive conducting polymer in a nanostructured architecture. However, no systematic study has been done so far to elucidate the underlying reasons behind this improvement.[18−20] One of the main obstacles is the lack of scalable processing methods that can effectively integrate ultrathin polymers conformally inside nanostructured electrodes with high porosity and tortuosity. *In situ* liquid synthesis through electrochemical polymerization though possible is constrained by mass transfer limitations and solvent interactions and is not easily scalable. Here, we propose oxidative chemical vapor deposition (oCVD) as a viable means for conformally coating porous carbon nanostructures to create enhanced charge capacity as pseudocapacitors. As a thin film deposition technique, oCVD has shown to be a viable route for the liquid-free synthesis of conducting polymers.[21−25] Of particular advantage is the ability of oCVD to synthesize and make use of intractable and insoluble conducting polymers. For example, unsubstituted polythiophene is among the most challenging conjugated polymer to work with as chains longer than eight units are practically insoluble and make the processing of this material near impossible. But polythiophene is an important energy storage material being both thermally and chemically stable and can go through both n-and p-doping repeatedly.[3] Recently, we have shown oCVD as a viable route for the synthesis and thin film formation of unsubstituted polythiophene.[26] By flowing vapors of the thiophene monomer and a strong enough oxidant such as vanadium oxytrichloride ($VOCl_3$) into a low pressure CVD reactor, the solid polymer thin film could be formed spontaneously on a substrate surface. The polymerization is a step growth process that is believed to follow an oxidative mechanism that allows the dehydrocoupling of heterocyclic rings.[27] Simultaneously, the deposited polymer is doped to its conductive form with counterions like chloride that are contributed by the oxidant.[28] By tuning oCVD synthesis conditions, we were able to systematically control polymer conjugation length and film electrical conductivity in the mS/cm range.[26] Here, oCVD is demonstrated as a facile and scalable approach to enable simultaneously the polymerization and thin film deposition of unsubstituted polythiophene for the purpose of creating enhanced pseudocapacitors. By using a new oxidant, antimony pentachloride ($SbCl_5$), we achieved unsubstituted polythiophene with conductivity as high as 70 S/cm. We found that polythiophene can store more specific charge compared to the theoretical limit set for the bulk material when the polymer is in the form of an ultrathin coating within a porous nanostructure. As a result, we were able to create pseudocapacitors with enhanced charge storage that is 2.5 fold higher than a conventional supercapacitor and with respectable stability up to 5000 cycles.

RESULTS AND DISCUSSION

The goal was to utilize the oCVD process for the deposition of conjugated polymer thin films within porous nanostructures to enable us to study the charge storage of electrochemically active polymers in confined nanostructures. The simultaneous oCVD polymerization and thin film formation of unsubstituted polythiophene was carried out in a laminar flow CVD reactor using thiophene and antimony pentachloride ($SbCl_5$) as the monomer and oxidant, respectively. The range of oCVD conditions of precursor flow rates, reactor pressure, and substrate temperature was examined carefully to identify the window in which the polymerization reaction was limiting, particularly important with deposition within porous nanostructured substrates, to maximize the diffusion of reactive species to the surface.

The oCVD synthesized polythiophene films adhered well to the underlying substrates, and none of the common solvents we tested, including tetrahydrofuran, chloroform, methanol, and methyl formamide, were able to dissolve the films. Nevertheless, washing the samples helped with removing the oxidant residue and dedoping of the film. As seen in Figure 1a, the

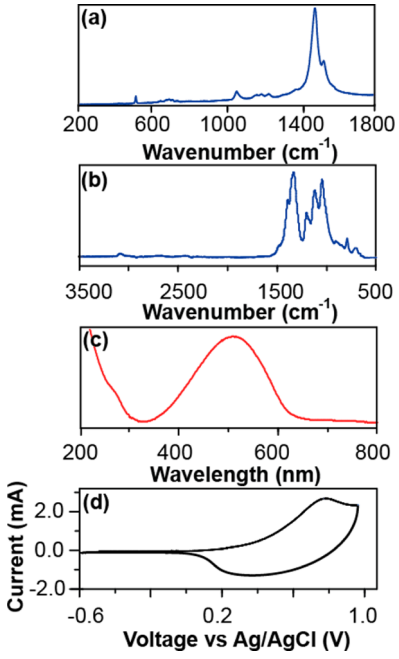

Figure 1. Characteristics of polythiophene synthesized by oCVD using thiophene monomer and antimony pentachloride oxidant. (a) Raman spectrum of an as-deposited doped film on silicon acquired with a 488 nm laser. (b) FTIR spectrum of an as-deposited doped film on silicon. (c) UV−vis spectrum of an as-deposited doped film on quartz, which has been dedoped. (d) Cyclic voltammogram of an as-deposited film on FTO glass.

Raman spectrum of an as-deposited film acquired with a 488 nm laser has the fingerprint expected of polythiophene with a high degree of polymerization and a correspondingly high conductivity of 50−70 S/cm.[29] Since oCVD enables the simultaneous doping of conjugated polymers through the oxidant during film deposition to yield the conductive doped form, Raman spectra acquired with a 633 nm laser were further used to investigate the dependence of film structure on resulting electrical conductivity, see Supporting Information Figure S1. The left shift of the quinoid peak (~1420 cm^{-1}) as shown in Supporting Information Figure S2 in the samples deposited by varying oCVD processing conditions (in this case reducing oxidant flow rate with all other conditions unchanged) matches the increase in film electrical conductivity, which agrees with our observations previously.[30] Figure 1b shows the Fourier transform infrared (FTIR) spectrum of an as-deposited film resembling that of polythiophene in its doped form, with significant doping induced vibrations broadening the C−C stretch region around 1100−1500 cm^{-1}.[31] However, the CH bending and stretching modes of polythiophene around 800 and 3000 cm^{-1}, respectively, are observable. As shown in Figure 1c, the UV−vis spectrum of an as-deposited film after dedoping the film to its undoped form (by exposure to 2.0 M methylamine in methanol for 2 min followed by washing with neat methanol) shows an absorption peak (λ_{max}) around 510 nm that corresponds to an appreciable conjugation length. By adjusting the reactant concentration in oCVD, λ_{max} of the resulting films could be blue-shifted by as much as 40 nm with a corresponding lowering of film conductivity, indicating we have good control over the polymer conjugation length. Figure 1d shows the cyclic voltammogram of an as-deposited polythiophene film measured in an electrolyte of 0.5 M tetraethylammonium tetrafluoroborate ($TEABF_4$) in acetonitrile. The p-doping (oxidation) and dedoping (reduction) peaks are clearly observed at 0.8 and 0.25 V *vs* Ag/AgCl, respectively, and are accompanied by a color change from red in the undoped state to deep blue in the doped form. The locations of these peaks match reported values of p-doping and dedoping peaks for unsubstituted polythiophene.[32]

Because of the insolubility of polythiophene in common solvents, the typical methods to measure polymer molecular weight, *e.g.*, by gel permeation chromatography (GPC) or solution viscometry, were not possible. Qualitatively, the Raman and UV spectra in Figure 1 indicate that the polythiophene has a degree of conjugation greater than several monomer repeat units long. As a more quantitative measure, FTIR was used to determine the degree of polymerization, which has been found to correlate with the ratio of the intensity of the IR bands at 690 and 790 cm^{-1},[29] giving an estimate in the range of 26−29 thiophene units. With the use of a transition metal halide oxidant to enable oxidative polymerization of thiophene, the oxidant has been found to also complex with the polymer during film growth, which leads to doping of the polythiophene and the observed electrical conductivity.[26] This is evidenced by the presence of antimony and chlorine within the as-deposited film from spectral data (see Supporting Information). However, washing of the films with tetrahydrofuran (THF) or methanol helped to remove the oxidant completely and consequently leads to dedoping of the polythiophene and a corresponding loss in electrical conductivity.[26] It should be noted that although the doped form of the polythiophene is characterized here by Raman and FTIR spectroscopy to reveal the level of doping (see Figure 1 discussion), the electrochemical measurements presented hereon are solely on the dedoped form of the polythiophene after thorough solvent washing to remove any trace of the antimony oxidant. This eliminates any effect or interference the oxidant might have on these subsequent measurements.

Chemical vapor deposition is well-known to produce conformal coatings on topographically complex substrates. Even with porous structures where the aspect ratio (length-to-diameter) of the pores can exceed 1000:1 and pore sizes are on the nanometer scale, CVD is able to achieve uniform and conformal coating on the pore walls, and if so desired, the pore spaces can even be entirely filled.[33,34] Here, we demonstrate a unique way to integrate unsubstituted polythiophene within porous nanostructures with exceptional control over film thickness and coating conformality by simple adjusting of oCVD synthesis parameters. We have chosen to deposit within anodized aluminum oxide (AAO) membranes having well-defined pore geometries in order to investigate the oCVD parameter space that leads to effective polymer integration. By reducing total pressure and oxidant concentration so as to be in the reaction-limited regime that favors mass transport inside the pores, we obtained conformal growth of the polymer within porous nanostructures with average deposition rates as low as 0.5 nm/min (deposition rate was estimated by taking the ratio of film thickness measured by cross-sectional SEM and film deposition time). Figure 2 shows 57 μm thick AAO membranes with a nominal pore diameter of 200 nm, comparing the white uncoated membrane (Figure 2a) to the polythiophene coated one which in the as-deposited doped form has a dark grayish blue color (Figure 2b), and the polythiophene coated disc after dedoping to yield the orange-red undoped state (Figure 2c). Cross-sectional scanning electron microscopy (SEM) images show that the vertically aligned pore channels of the AAO membrane (Figure 2d) have been conformally coated with polythiophene, in this case with a film thickness of ~30 nm (Figure 2e). This uniform coating is

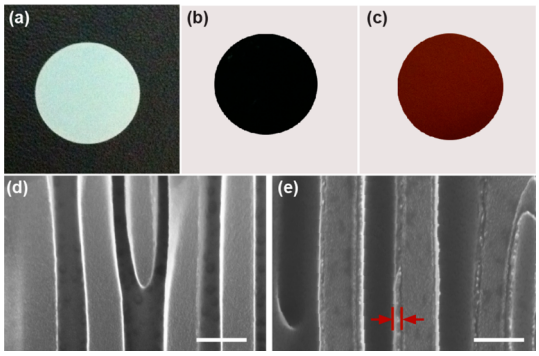

Figure 2. Conformal coating of polythiophene within porous nanostructures using oCVD. (a) Uncoated anodized aluminum oxide (AAO) membrane, 57 μm thick and 200 nm pore diameter. (b) Polythiophene coated AAO in the as-deposited doped state of the polymer. (c) Polythiophene coated AAO in the undoped state of the polymer after dedoping. (d) Cross-sectional SEM of an AAO membrane showing the porous channels (darker shade). (e) Cross-sectional SEM of a polythiophene coated AAO membrane showing conformal and uniform coating along the pore walls (coating thickness noted by the red arrows). Scale bars in the SEM images are 200 nm.

observed throughout the entire thickness of the AAO membrane, see Supporting Information Figure S3, and demonstrates oCVD's ability to create conformal films along pore walls inside porous nanostructures by manipulating the rate of polymerization at the surface relative to mass transport dynamics. The presence of polythiophene all the way through the AAO membrane thickness was confirmed by performing energy dispersive X-ray spectroscopy (EDS) over the cross section of AAO disk coated with polythiophene. The concomitant presence of aluminum and sulfur of uniform signal intensity along the cross section suggests a well controlled coating along the wall within the nanopores, see Supporting Information Figure S4. In contrast, under faster reaction conditions at higher oxidant flow rates, preferential deposition on the outer membrane surface rather than inside the pores led to nonconformal coating and eventually premature pore blockage, see Supporting Information Figure S5.

With the ability to create conformal coatings inside porous nanostructures, we turned our focus to study the effect of a porous nanostructure on the electrochemical behavior of polythiophene films. Here, oCVD was used to deposit polythiophene films on planar FTO substrates as well as inside 4 μm mesoporous TiO_2 layers supported on FTO substrates. The TiO_2 layers consisted of a network of 25 nm TiO_2 interconnected nanoparticles spin coated from a suspension onto FTO glass and annealed at 450 °C to remove the solvent, resulting in a mesoporous network structure. Conformal coating inside mesoporous layers as thick as 4 μm as evidenced by EDS mapping over the cross section of TiO_2 layer (see Supporting Information Figure S6) was obtained at a slow deposition rate of 1 nm/min (based on estimating an average film thickness by knowing the mass of deposited polymer, the total available substrate surface area, and assuming a polymer density, see below).[43] Cyclic voltammetry was used to derive the specific capacitance of the polymer using the following equation:

$$C_{sp} = \frac{1}{\alpha m}\frac{\int i\,dV}{\Delta V} \quad (1)$$

where α is the scan rate, m only considers the mass of the polymer, i and V are the current and voltage on the voltammogram, and ΔV is the window over which cyclic voltammetry was performed. The TiO_2 porous layer itself was found to contribute minimal capacitance (<1 F/g) so the capacitance measurements are expected to only probe the effect of the polymer.

Figure 3a gives the specific capacitance (per mass of the polymer) for polythiophene thin films deposited on planar substrates and inside mesoporous TiO_2 nanostructures. Clearly, there is a dependence of the specific capacitance on polymer thickness both on the planar substrate (250 and 800 nm) and within the nanostructure (4 and 6 nm). Film thickness of polythiophene on the flat substrates was measured directly through cross-sectional SEM while that inside the nanostructures was estimated by measuring the mass gain due to the polymer after oCVD using thermogravimetric analysis (TGA) and relating it to polythiophene density (1.2 g/cm^3) and the nanostructure specific surface area (55 m^2/g$_i$).[34,35] For polythiophene deposited on planar substrates, the specific capacitance of thin films (down to 25 nm as the minimum film thickness practically possible for electrochemical measurements) over the 1.5 V window was found to be 150 F/g and for thicker samples (>450 nm) this value was reduced to 75 F/g. To understand this difference, the anodic peak current taken from the cyclic voltammogram was traced as a function of scan rate, see Figure 3b. For a planar thin film (250 nm), the linear response is characteristic of a reaction limited behavior in the redox process. In contrast for a thick film (800 nm), the deviation from a linear response indicates that ion diffusion and penetration inside the polymer becomes limiting. This is confirmed by the linear relationship obtained by plotting the peak current with the square root of the scan rate predicted for the ion diffusion limited case, and which allows an estimate of the BF_4^- ion diffusion coefficient of 8.9×10^{-9} m^2/s to be obtained from solving the diffusion equation under semi-infinite conditions that yields an equation relating peak current with scan rate

$$I_p = (2.69 \times 10^5)n^{3/2}AcD^{1/2}\nu^{1/2} \quad (2)$$

where I_p is the peak current (amps), n is the number of electrons transferred, A is the electrode surface area (cm^2), c is the salt concentration (mol/cm^3), D is the ion diffusion coefficient (cm^2/s), ν is the scan rate (V/s),

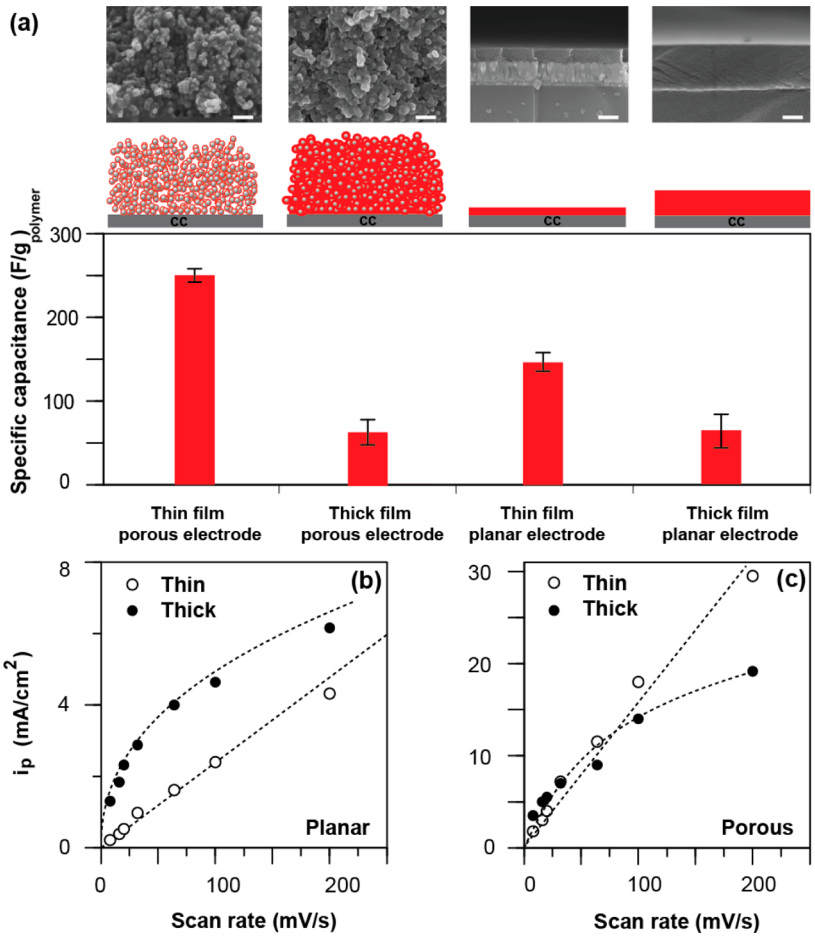

Figure 3. Effect of polymer thickness and 3D nanostructure on the specific capacitance of oCVD polythiophene. (a) SEM images (scale bar is 200 nm) and specific capacitance values of thin (250 nm) and thick (800 nm) films on planar FTO electrodes, and of thin (~4 nm) and thick (~6 nm) films inside mesoporous electrodes of TiO_2; specific capacitance is based on per mass of polymer and reported with 2 standard deviations. The current density of the anodic (doping) peak as a function of scan rate for different thickness of films on (b) planar substrates and (c) within mesoporous nanostructures.

and the proportionality constant is $0.4463(F^3/RT)^{1/2}$ ($C^{3/2}$ mol^{-1} $J^{-1/2}$) in which F (96485.33 C/mol) is Faraday's constant, R (8.314 J mol^{-1} K^{-1}) is the gas constant and T (300 K) is the temperature of measurement.[36] This value is in the range of diffusion coefficient values reported for thiophene polymers in planar geometry.[37] The difference in specific capacitance between thin and thick polythiophene films is also seen for the case of the polymer deposited within the mesoporous TiO_2 nanostructures. As the polymer thickness increased from 4 to 6 nm, the latter being close to the limit at which the pores become filled, the specific capacitance was significantly reduced from 250 to 75 F/g, see Figure 3a. By plotting the anodic peak current as a function of scan rate, as seen in Figure 3c, again the thicker coating this time within the nanostructure shows that the redox process is highly diffusion limited. Plotting the current with the square root of the scan rate yields a linear behavior for the ion diffusion limited process, leading to a diffusion coefficient for BF_4^- ions to be 8.2×10^{-8} m^2/s, which is an order higher than that for the dense, thick planar polythiophene film but is comparable to that reported for the diffusion of ions in a liquid electrolyte within nanoporous electrodes.[38] This suggests that diffusion in this case is limited by ion diffusion in the liquid and not in the polymer, presumably due to the much narrower pore channels with the thicker polymer coating inside the porous nanostructure.

What is more important with the results in Figure 3a is the significant enhancement in specific capacitance when a thin polythiophene film is inside the mesoporous TiO_2 layer compared to a thin film on a planar substrate, where in both cases ion diffusion is not limiting. If the thin polythiophene film inside the nanostructure were solely dictated by reaction controlled redox processes, then the expected specific capacitance (per mass of polymer) should be similar to that of the thin planar film. However, the measured capacitance for the film inside the porous nanostructure is almost 1.6 times higher. The data suggests that the three-dimensional nanostructured pore surface adds a significant component to the electrochemical behavior of polythiophene that is not available on a

two-dimensional planar surface. There are reports to indicate that a nanoconfinement effect can significantly increase the electrical double layer capacitance (EDLC) in nanoporous electrodes. This has been attributed to enhanced collision frequency of ions with the pore walls as ions diffuse within a porous media (analogous to gas phase Knudsen transport) as well as enhanced charge screening with the electric field distribution inside the nanoporous structure.[39] This increase in double layer capacitance due to nanoconfinement has been shown to be a strong function of roughness (defined as the ratio of actual to geometric surface area) and ion concentration in the bulk.[40] There is the possibility that the polythiophene might have a double layer capacitance component that could lead to the nanoconfinement enhanced capacity as observed in other double layer nanoporous structures[41,42] since we see a flat rectangular portion in the cyclic voltammograms (see Supporting Information Figure S7) that suggest some double layer contribution. It is also possible that the faradaic processes in polythiophene could be augmented in a nanoconfined polymer. The increase in faradaic current could arise from more stable and reversible oxidation of the polymer. In the bulk, further oxidation can be achieved at higher electrode potentials; however, in the case of unsubstituted polythiophene this easily leads to overoxidation in the presence of solvent nucleophiles that results in irreversible polymer degradation.[43,44] However, with the polymer confined in the nanopores, more oxidation could potentially be achieved without irreversible chemical degradation since the pores might hinder nucleophiles present in the bulk solution from interacting with the polymer.[16,39,45] For our case, the enhanced charge capacity most likely comes from both additional faradaic contributions and double layer capacitance of the polythiophene rather than solely from an electrical double layer (it should be noted that the bare TiO_2 nanostructure had negligible measurable capacitance). Although it is possible that the much smaller thickness of polythiophene within the nanopores compared to that on a planar substrate might itself lead to the observed increase in capacity (rather than any effect attributed to pore confinement), we believe that this is not the case based on the fact that we did not see any thickness dependency on the specific capacitance of the polymer on a planar substrate for coating thickness in the range of 25−450 nm where ion diffusion is not limiting. We believe that the observed augmentation of the specific capacitance of the polymer within the nanoporous electrode is most likely related to the nanostructural template where the template contribution itself to the total electrode capacitance is insignificant.

Given the ability to significantly enhance charge storage with ultrathin oCVD polythiophene within porous TiO_2 nanostructures, we investigated further by using oCVD to integrate polythiophene thin films within the nanostructure of activated carbon electrodes to create pseudocapacitor devices. Unsubstituted polythiophene was conformally coated within the porous activated carbon by oCVD at various deposition times using a constant set of oCVD deposition conditions (1 Torr pressure, 0.3 sccm oxidant flow rate, 2.5 sccm monomer flow rate, and 30 °C substrate temperature) to obtain electrodes with different mass loadings of the polymer within the matrix. Figure 4a−d shows the top-down SEM images of the activated carbon particles in the fabricated electrodes before and after oCVD with several mass loadings of polymer to activated carbon (1:1, 1.5:1, and 2.7:1). As seen in Figure 4a, uncoated activated carbon particles have a very rough surface consisting of microscale topologies and mesopores. With an increasing amount of polythiophene as in Figure 4b,c, the surface morphology becomes noticeably smoother, and eventually at high enough loading of the polymer as in Figure 4d the coating is sufficient to cover the microscale features and fill in many of the pores. As shown in Supporting Information Figure S8, the STEM image of a microtomed section of a lightly coated activated carbon electrode shows the polymer is present inside the porous particle and not only on the outer surface, which again demonstrates the utility of oCVD in integrating ultrathin polythiophene within porous nanostructures. As shown in Figure 4e, specific capacitance values of oCVD polythiophene coated activated carbon pseudocapacitors are highly dependent on the mass loading of polymer. In particular, at a polymer-to-activated carbon mass ratio of ∼1.5, specific capacitance reaches a maximum, a value ∼50% higher than that for bare activated carbon (145 *vs* 92 F/g). More significantly, this capacitance translates to over a 250% increase in volumetric capacitance since the volume contribution of the ultrathin polymer coating is negligible (120 *vs* 47 F/cm^3). Figure 4f shows cyclic voltammetry sweeps of the polythiophene coated activated carbon at the 1.5:1 mass ratio over a 4.0 V window at different scan rates. The dependency of the peak current value upon the scan rate is not entirely linear, but there is no sign of diffusion limitations up to 100 mV/s. The pseudocapacitor is shown to be stable up to the 5000 cycles tested with a small 10% capacitance drop during the first 100 cycles, see Figure 4g.

Looking back at each cyclic voltammogram in Figure 4f, we observe that the signal has both characteristics of a pure electrical double layer capacitor (EDLC) and faradaic processes associated with a pseudocapacitor. The flat portion of the curves around 0 V is characteristic of the rectangular plot typically obtained with an EDLC such as activated carbon, while the peaks noticeable toward either edge of the voltage window relate to the redox reactions of a pseudocapacitor like polythiophene. This suggests that the ultrathin polythiophene coating did not completely block access to

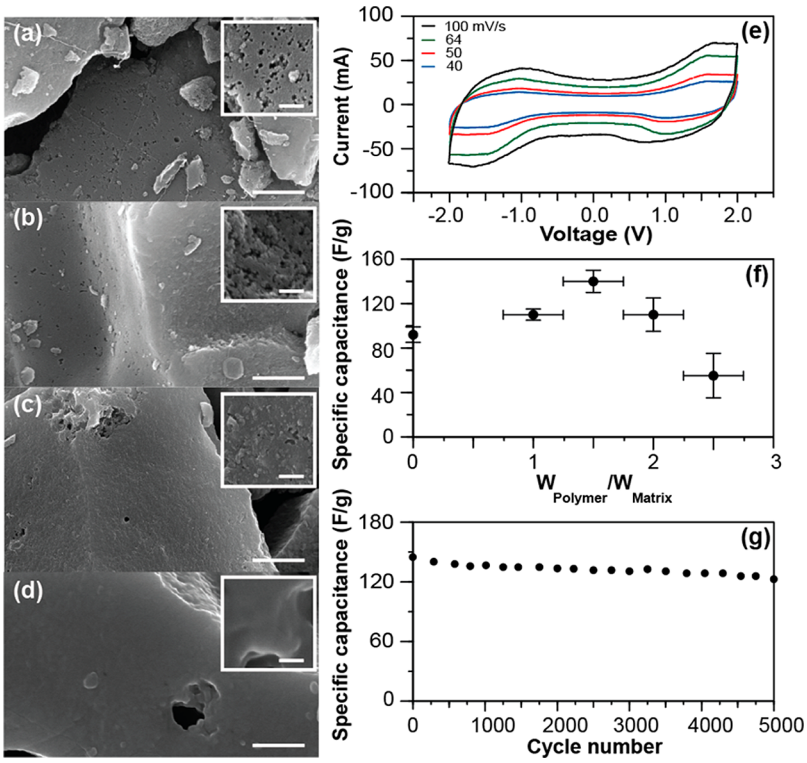

Figure 4. Electrochemical behavior of oCVD polythiophene coated activated carbon. SEM images of activated carbon electrodes (a) without coating and coated with polythiophene at polymer-to-activated carbon mass ratios of (b) 1:1, (c) 1.5:1, and (d) 2.7:1 (insets show a magnified region of the surface morphology of each sample; scale bar is 1 μm and 50 nm for the inset). (e) Cyclic voltammograms of the 1.5:1 mass ratio pesudocapacitor recorded at different scan rates between -2 and $+2$ V. (f) Specific capacitance values based on per total mass of electrode for different polymer mass loadings. Measurements were made at 100 mV/s for five different samples at each loading with the error bars representing two standard deviations. (g) Capacitance of the same sample measured up to 5000 cycles (at 100 mV/s).

pores so that a considerable portion of the activated carbon surface is still available for ions to dock at the surface and contribute to charge storage in electrical double layers. This area could be mainly from the micropores that are inaccessible to oCVD for conformal polymer coating, and therefore, activated carbon remains accessible to ions. However, when the polymer coating becomes too thick, these pores no longer become accessible, and further, the surface features in activated carbon become more rounded and ill-defined. This could lead to lower capacitance due to pore blockage, less surface area and even the onset of diffusion limitations. This could explain the behavior observed in Figure 4e, in which the maximum capacitance observed with polymer mass loading could be understood as an initial increase in the contribution from pseudocapacitance with having more redox active polymer to an eventual decrease in capacitance due to a drop in surface area and pore blocking with thicker polymer coatings.

The enhanced capacitance observed with thinner polymer films in TiO_2 nanostructures as well as the optimal polymer loading for maximizing capacitance seen with the activated carbon electrodes indicate that care must be taken when designing and optimizing electrodes that integrate electroactive materials. The design should be one where a sufficient wall-to-wall distance (in the sub-10 nm range) is available to guarantee the electrical double layer action and maintain perm-selectivity, ion diffusion and access to the pores. Any volume expansion of the electrode and electroactive polymer materials during charging must be considered to avoid pore blockage, mass transfer limitations, and the loss of the double layer.

CONCLUSIONS

We have demonstrated oCVD's unique ability to synthesize unsubstituted polythiophene based on the direct vapor-to-solid oxidative polymerization of thiophene monomer using antimony pentachloride oxidant. Ultrathin polythiophene films have been successfully integrated within high aspect ratio porous nanostructures of AAO, TiO_2 and activated carbon by operating oCVD under slow kinetics that favor reactant mass transport. Significantly, ultrathin conformal polythiophene coatings that preserve the high surface area of the porous nanostructures showed enhanced capacitance 1.6 times over that of planar films that could be attributed to nanoconfinement effects not available in open planar geometries. As a result, type I symmetric pseudocapacitors consisting of polythiophene coated activated carbon electrodes displayed significantly

greater energy storage capacity compared to bare activated carbon, with an increase of 50 and 250% in specific and volumetric capacitance, respectively, at an optimal polymer-to-activated carbon mass ratio of 1.5:1. Capacitance was stable up to the 5000 cycles tested with a small decrease of 5% within the first 100 cycles. The capacitance enhancement could be attributed to the preservation of nanostructure surface area and accessible pore space that is afforded by ultrathin films. oCVD promises to be a valuable synthesis and processing pathway for making conductive polymers and creating enhanced energy storage solutions that takes advantage of nanostructured device architectures.

METHODS

oCVD Synthesis of Unsubstituted Polythiophene. To enable the oCVD polymerization of unsubstituted polythiophene, thiophene monomer (Aldrich, 97%) and antimony pentachloride oxidant (Acros Organics, 95%) were used as received. Vapors of thiophene and antimony pentachloride were generated by mild heating of the source liquids to 35 °C, and metered into the CVD reactor through precision needle valves to achieve flow rates of 2.0−5.0 and 0.1−1.0 sccm (standard cm^3 per min), respectively. Total pressure in the reactor was automatically maintained at set points in the range of 0.5−1.5 Torr using a downstream throttle valve, while substrate temperature was controlled in the range of 25−30 °C using backside contact with a recirculating thermal fluid. Polymer synthesis and film deposition were performed on various substrates, including planar silicon, fluorine-doped tin oxide (FTO) glass (Hartford Glass), mesoporous TiO_2 nanoparticle layers on FTO using previously published methods,[34] and activated carbon on either FTO or stainless steel plates (see below).

Polymer Film Characterization. Fourier transform infrared (FTIR) spectra were acquired on a Thermo Nicolet 6700 spectrometer in normal transmission mode using an MCT/A detector at a resolution of 4 cm^{-1} averaged over 64 scans. UV−vis spectra of deposited films on quartz glass were acquired jn the range of 280−800 nm with 1 nm resolution using a Shimadzu UV-1700 spectrophotometer. Raman spectra were collected on a Renishaw RM1000 microspectrometer using either a 488 nm Ar ion laser 488 nm with ∼1 μm lateral spot size and 11 mW total power or a 633 nm He−Ne laser with ∼2 μm lateral spot size and 20 mW total power. Film conductivity was estimated through measuring sheet resistivity from an Alessi four-point probe connected to a Keithley 2400 source meter and film thickness from cross-sectional SEM averaged over 5 different locations along the same line as the four-point probe pins.

Activated Carbon Electrode Fabrication. The activated carbon mat was fabricated according to published protocol using YP-50 particles (Kuaray Chemical, average particle size 5−15 μm, 1500−1800 cm^2/g specific surface area with nominal pore size of 0.5−2 nm) and 5.0% binder (60 wt % PTFE suspension in water) to obtain 100 μm thick electrodes.[46] The mat was cut into 1 cm^2 size for oCVD coating and electrochemical characterization.

Thickness Estimation. The thickness of the polymer within porous nanostructures was estimated based on the mass of deposited polythiophene within the electrodes. The polymer mass was measured by TGA analysis after soaking each sample for a day in methanol to remove any antimony oxidant residue followed by drying in air for at least 1 h. To calculate the polymer film thickness, the polymer was assumed to be spread uniformly within the porous electrode and the density of polythiophene was taken as 0.92 g/cm^3 based on blanket thick film deposition. Total surface area of the nanostructured electrode was estimated using the TiO_2 electrode matrix weight measured from the final plateau value of the TGA curve and the specific area of the TiO_2 electrode derived from N_2 adsorption isotherms (a_{BET} ∼55 m^2/g). Using the total electrode surface area and the mass and density of the deposited polymer, the thickness was back calculated. For the planar samples, film thickness was measured using SEM along the cross section of the sample and averaged over 5 different positions.

Polymer Integration within Nanostructured Electrodes. Polythiophene was integrated within various porous nanostructures, including anodized aluminum oxide (AAO) disks (Whatman, 0.2 μm pore size and 60 μm thickness), mesoporous titanium dioxide coated on FTO glass (20 nm nominal pore size and 4 μm thickness), and activated carbon electrodes. The oCVD deposition conditions were tuned for different substrates to achieve conformal coating that was evaluated based on SEM imaging and gravimetric analysis, assuming constant density for polythiophene of 0.92 g/cm^3 estimated from blanket thick film deposition. Optimal conditions were found when total pressure was set at 500 mTorr and the substrate temperature was kept constant at 30 °C. For the AAO membranes, flow rates of thiophene and antimony chloride were 2.0 and 0.1 sccm, respectively. For the mesoporous TiO_2 electrodes, flow rates were 5.0 and 0.2 sccm, respectively, and for the activated carbon electrodes, flow rates were 4.0 and 0.2 sccm. Nitrogen was used as an inert patch flow to keep the total flow rate fixed at 5 sccm.

Capacitance Measurements. Before performing any electrochemical tests, the samples were soaked in tetrahydrofuran (THF) for 3 h to clean the surface and dried in a vacuum oven for 8 h to remove the THF completely. The electrochemical charge storage capacity of the polymer films deposited on planar electrodes and within porous nanostructured electrodes was then investigated in a three electrode setup using cyclic voltammetry. Voltage was swept over a potential window of 1.5 V (−0.5 to +1.0 V) *vs* Ag/AgCl in a liquid electrolyte of 0.5 M $TEABF_4$ in acetonitrile and using an oversized activated carbon as the counter electrode. The electrochemical performance of the activated carbon electrodes after polythiophene dedoping, THF washing, and drying were tested in a symmetric two electrode Swagelok cell using 1 M $TEABF_4$ in acetonitrile as the electrolyte.[47] A voltage range of −2 to +2 V was found to be an appropriate window over which the fabricated electrodes were stable (this was based on separate cyclic voltammetry measurements made beforehand in a three electrode setup where the electrodes were used in a symmetric configuration and the voltage on the electrode was probed independently *vs* an Ag/AgCl electrode).[48] Specific capacitance of the assembled Swagelok cells was derived from cyclic voltammetry using the total mass of the electrode (including the polymer, activated carbon and binder).

Conflict of Interest: The authors declare no competing financial interest.

Supporting Information Available: Further Raman spectra of polythiophene films deposited on silicon, SEM images and EDX spectra of polythiophene coated within porous nanostructures, and cyclic voltammograms of nanostructured electrodes integrated with polythiophene. This material is available free of charge *via* the Internet at http://pubs.acs.org.

Acknowledgment. This work was supported by the National Science Foundation (CAREER CBET-0846245, CBET-0820608, and CBET-1264487). The authors would like to thank Y. Choo at Yale University for the STEM measurements. We also acknowledge the use of Drexel University's Centralized Research Facilities.

REFERENCES AND NOTES

1. Laforgue, A.; Simon, P.; Sarrazin, C.; Fauvarque, J. F. Polythiophene Based Supercapacitor. *J. Power Sources* **1999**, *80*, 142–148.

2. Liu, D. Y.; Reynolds, J. R. Dioxythiophene-Based Polymer Electrodes for Supercapacitor Modules. *ACS Appl. Mater. Interfaces* **2010**, *2*, 3586–3593.
3. Rudge, A.; Raistrick, I.; Gottesfeld, S.; Ferraris, J. P. A Study of the Electrochemical Properties of Conducting Polymers for Application in Electrochemical Capacitors. *Electrochim. Acta* **1994**, *39*, 273–287.
4. Conway, B. E. *Electrochemical Supercapacitors: Scientific Fundamentals and Technological Applications*; Plenum: New York, 1999; pp 259−284.
5. Simon, P.; Gogotsi, Y. Materials for Electrochemical Capacitors. *Nat. Mater.* **2008**, *7*, 845–854.
6. Lee, S. W.; Kim, J.; Chen, S.; Hammond, P. T.; Shao-Horn, Y. The Influence of Transition Metal Oxides on the Kinetics of Li_2O_2 Oxidation for Li-O_2 Batteries: High Activity of Chromium Oxides. *ACS Nano* **2010**, *4*, 3889–3896.
7. Fischer, A. E.; Pettigrew, K. A.; Rolison, D. R.; Stroud, R. M.; Long, J. W. Incorporation of Homogeneous, Nanoscale MnO_2 Within Ultraporous Carbon Structures *via* Self-Limiting Electroless Deposition: Implications for Electrochemical Capacitors. *Nano Lett.* **2007**, *7*, 281–286.
8. Ertas, M.; Walczak, R. M.; Das, R. K.; Rinzler, A. G.; Reynolds, J. R. Supercapacitors Based on Polymeric Dioxypyrroles and Single Walled Carbon Nanotubes. *Chem. Mater.* **2012**, *24*, 433–443.
9. Fan, L. Z.; Hu, Y. S.; Maier, J.; Adelhelm, P.; Smarsly, B.; Antonietti, M. High Electroactivity of Polyaniline in Supercapacitors by Using a Hierarchically Porous Carbon Monolith as a Support. *Adv. Funct. Mater.* **2007**, *17*, 3083–3087.
10. Khomenko, V.; Frackowiak, E.; Béguin, F. Determination of the Specific Capacitance of Conducting Polymer/Nanotubes Composite Electrodes Using Different Cell Configurations. *Electrochim. Acta* **2005**, *50*, 2499–2506.
11. Lota, K.; Khomenko, V.; Frackowiak, E. Capacitance Properties of Poly(3,4-Ethylenedioxythiophene)/Carbon Nanotubes Composites. *J. Phys. Chem. Solids* **2004**, *65*, 295–301.
12. Wang, K.; Huang, J.; Wei, Z. Conducting Polyaniline Nanowire Arrays for High Performance Supercapacitors. *J. Phys. Chem. C* **2010**, *114*, 8062–8067.
13. Zhang, J.; Kong, L. B.; Wang, B.; Luo, Y. C.; Kang, L. *In-Situ* Electrochemical Polymerization of Multi-Walled Carbon Nanotube/Polyaniline Composite Films for Electrochemical Supercapacitors. *Synth. Met.* **2009**, *159*, 260–266.
14. Xu, J.; Wang, K.; Zu, S. Z.; Han, B. H.; Wei, Z. Hierarchical Nanocomposites of Polyaniline Nanowire Arrays on Graphene Oxide Sheets with Synergistic Effect for Energy Storage. *ACS Nano* **2010**, *4*, 5019–5026.
15. Ambade, R. B.; Ambade, S. B.; Shrestha, N. K.; Nah, Y. C.; Han, S. H.; Lee, W.; Lee, S. H. Polythiophene Infiltrated TiO_2 Nanotubes as High-Performance Supercapacitor Electrodes. *Chem. Commun.* **2013**, *49*, 2308–2310.
16. Peng, C.; Zhou, X.; Chen, G. Z.; Moggia, F.; Fages, F.; Brisset, H. Roncali, Internally Referenced Analysis of Charge-Transfer Reactions in A New Ferrocenyl Bithiophenic Conducting Polymer through Cyclic Voltammetry. *Chem. Commun.* **2008**, 6606–6608.
17. Peng, C.; Hu, D.; Chen, G. Z. Theoretical Specific Capacitance Based on Charge Storage Mechanisms of Conducting Polymers: Comment on Vertically Oriented Arrays of Polyaniline Nanorods and Their Super Electrochemical Properties. *Chem. Commun.* **2011**, *47*, 4105–4107.
18. Park, J. H.; Ko, J. M.; Park, O. O.; Kim, D. W. Capacitance Properties of Graphite/Polypyrrole Composite Electrode Prepared by Chemical Polymerization of Pyrrole on Graphite Fiber. *J. Power Sources* **2002**, *105*, 20–25.
19. Wang, H.; Hao, Q.; Yang, X.; Lu, L.; Wang, X. A Nanostructured Graphene/Polyaniline Hybrid Material for Supercapacitors. *Nanoscale* **2010**, *2*, 2164–2170.
20. Zhang, K.; Zhang, L. L.; Zhao, X. S.; Wu, J. Graphene/Polyaniline Nanofiber Composites as Supercapacitor Electrodes. *Chem. Mater.* **2010**, *22*, 1392–1401.
21. Tenhaeff, W. E.; Gleason, K. K. Initiated and Oxidative Chemical Vapor Deposition of Polymeric Thin Films: iCVD and oCVD. *Adv. Funct. Mater.* **2008**, *18*, 979–992.
22. Alf, M. E.; Asatekin, A.; Barr, M. C.; Baxamusa, S. H.; Chelawat, H.; Ozaydin-Ince, G.; Petruczok, C. D.; Sreenivasan, R.; Tenhaeff, W. E.; Trujillo, N. J.; *et al.* Chemical Vapor Deposition of Conformal, Functional, and Responsive Polymer Films. *Adv. Mater.* **2010**, *22*, 1993–2027.
23. Asatekin, A.; Barr, M. C.; Baxamusa, S. H.; Lau, K. K. S.; Tenhaeff, W.; Xu, J.; Gleason, K. K. Designing Polymer Surfaces *via* Vapor Deposition. *Mater. Today* **2010**, *13*, 26–33.
24. Bhattacharyya, D.; Howden, R. M.; Borrelli, D. C.; Gleason, K. K. Vapor Phase Oxidative Synthesis of Conjugated Polymers and Applications. *J. Polym. Sci., Part B: Polym. Phys.* **2012**, *50*, 1329–1351.
25. Ozaydin-Ince, G.; Coclite, A. M.; Gleason, K. K. CVD of Polymeric Thin Films: Applications in Sensors, Biotechnology, Microelectronics/Organic Electronics, Microfluidics, MEMS, Composites and Membranes. *Rep. Prog. Phys.* **2012**, *75*, 016501.
26. Nejati, S.; Lau, K. K. S. Chemical Vapor Deposition Synthesis of Tunable Unsubstituted Polythiophene. *Langmuir* **2011**, *27*, 15223–15229.
27. Kovacic, P.; Jones, M. B. Dehydro Coupling of Aromatic Nuclei by Catalyst-Oxidant Systems: Poly (P-Phenylene). *Chem. Rev.* **1987**, *87*, 357–379.
28. Im, S. G.; Gleason, K. K. Systematic Control of the Electrical Conductivity of Poly(3,4-ethylenedioxythiophene) *via* Oxidative Chemical Vapor Deposition. *Macromolecules* **2007**, *40*, 6552–6556.
29. Furukawa, Y.; Akimoto, M.; Harada, I. Vibrational Key Bands and Electrical-Conductivity of Polythiophene. *Synth. Met.* **1987**, *18*, 151–156.
30. Shi, G. Q.; Xu, J. K.; Fu, M. X. Raman Spectroscopic and Electrochemical Studies on the Doping Level Changes of Polythiophene Films During their Electrochemical Growth Processes. *J. Phys. Chem. B* **2002**, *106*, 288–292.
31. Yamamoto, T.; Morita, A.; Miyazaki, Y.; Maruyama, T.; Wakayama, H.; Zhou, Z. H.; Nakamura, Y.; Kanbara, T.; Sasaki, S.; Kubota, K. Preparation of π-Conjugated Poly(thiophene-2,5-diyl), Poly(*p*-phenylene), and Related Polymers Using Zerovalent Nickel Complexes. Linear Structure and Properties of the π-Conjugated Polymers. *Macromolecules* **1992**, *25*, 1214–1223.
32. Waltman, R. J.; Bargon, J.; Diaz, A. F. Electrochemical Studies of Some Conducting Polythiophene Films. *J. Phys. Chem.* **1983**, *87*, 1459–1463.
33. Asatekin, A.; Gleason, K. K. Polymeric Nanopore Membranes for Hydrophobicity-Based Separations by Conformal Initiated Chemical Vapor Deposition. *Nano Lett.* **2010**, *11*, 677–686.
34. Nejati, S.; Lau, K. K. S. Pore Filling of Nanostructured Electrodes in Dye Sensitized Solar Cells by Initiated Chemical Vapor Deposition. *Nano Lett.* **2011**, *11*, 419–423.
35. Mo, Z.; Lee, K. B.; Moon, Y. B.; Kobayashi, M.; Heeger, A. J.; Wudl, F. X-ray Scattering from Poly(thiophene): Crystallinity and Crystallographic Structure. *Macromolecules* **1985**, *18*, 1972–1977.
36. Bard, A. J.; Faulkner, L. R. *Electrochemical Methods: Fundamentals and Applications*, 2nd ed.; Wiley: New York, 2001; p 231.
37. Kim, Y.; Kim, Y.; Kim, S.; Kim, E. Electrochromic Diffraction from Nanopatterned Poly(3-hexylthiophene). *ACS Nano* **2010**, *4*, 5277–5284.
38. Zuleta, M.; Björnbom, P.; Lundblad, A.; Nurk, G.; Kasuk, H.; Lust, E. Determination of Diffusion Coefficients of Inside Carbon Nanopores Using the Single Particle Microelectrode Technique. *J. Electroanal. Chem.* **2006**, *586*, 247–259.
39. Park, S.; Kim, H. C.; Chung, T. D. Electrochemical Analysis Based on Nanoporous Structures. *Analyst* **2012**, *137*, 3891–903.
40. Boo, H.; Park, S.; Ku, B.; Kim, Y.; Park, J. H.; Kim, H. C.; Chung, T. D. Ionic Strength-Controlled Virtual Area of Mesoporous Platinum Electrode. *J. Am. Chem. Soc.* **2004**, *126*, 4524–4525.
41. Chmiola, J.; Yushin, G.; Gogotsi, Y.; Portet, F.; Simon, P.; Taberna, P. L. Anomalous Increase in Carbon Capacitance

at Pore Sizes Less Than 1 Nanometer. *Science* **2006**, *313*, 1760–1763.
42. Huang, J.; Sumpter, B. G.; Meunier, V. Theoretical Model for Nanoporous Carbon Supercapacitors. *Angew. Chem., Int. Ed.* **2008**, *47*, 520–524.
43. Dietrich, M.; Heinze, J. Poly(4,4′-dimethoxybithiophene)—A New Conducting Polymer With Extraordinary Redox And Optical Properties. *Synth. Met.* **1991**, *41*, 503–506.
44. Zhou, H.; Chen, H.; Luo, S.; Lu, G.; Wei, W.; Kuang, Y. The Effect of the Polyaniline Morphology on the Performance of Polyaniline Supercapacitors. *J. Solid State Electrochem.* **2005**, *9*, 574–580.
45. Ofer, D.; Crooks, R. M.; Wrighton, M. S. Potential Dependence of the Conductivity of Highly Oxidized Polythiophenes, Polypyrroles, and Polyaniline: Finite Windows of High Conductivity. *J. Am. Chem. Soc.* **1990**, *112*, 7869–7879.
46. Chmiola, J. Pore-Size Ion-Size Correlations for Carbon Supercapacitors. Ph.D. Dissertation, Drexel University, Philadelphia, PA, 2009.
47. Beattie, S. D.; Manolescu, D. M.; Blair, S. L. High-Capacity Lithium-Air Cathodes. *J. Electrochem. Soc.* **2009**, *156*, A44–A47.
48. Lewis, T. W.; Spinks, G. M.; Wallace, G. G.; Mazzoldi, A.; De Rossi, D. Investigation of the Applied Potential Limits for Polypyrrole when Employed As the Active Components of a Two-Electrode Device. *Synth. Met.* **2001**, *122*, 379–385.